Anal Bioanal Chem
DOI 10.1007/s00216-013-7478-9

REVIEW

A critical evaluation of the current state-of-the-art in quantitative imaging mass spectrometry

Shane R. Ellis · Anne L. Bruinen · Ron M. A. Heeren

Received: 4 September 2013 / Revised: 28 October 2013 / Accepted: 31 October 2013

Abstract Mass spectrometry imaging (MSI) has evolved into a valuable tool across many fields of chemistry, biology, and medicine. However, arguably its greatest disadvantage is the difficulty in acquiring quantitative data regarding the surface concentration of the analyte(s) of interest. These difficulties largely arise from the high dependence of the ion signal on the localized chemical and morphological environment and the difficulties associated with calibrating such signals. The development of quantitative MSI approaches would correspond to a giant leap forward for the field, particularly for the biomedical and pharmaceutical fields, and is thus a highly active area of current research. In this review, we outline the current progress being made in the development and application of quantitative MSI workflows with a focus on biomedical applications. Particular emphasis is placed on the various strategies used for both signal calibration and correcting for various ion suppression effects that are invariably present in any MSI study. In addition, the difficulties in validating quantitative-MSI data on a pixel-by-pixel basis are highlighted.

Keywords Imaging mass spectrometry · Quantification · MALDI · SIMS · LA-ICP-MS · Ambient ionization

Introduction

Mass spectrometry imaging (MSI) has evolved into a multidisciplinary and indispensible tool for studying the spatial distributions of molecules within a diverse range of samples [1–4]. The most widespread uptake of MSI methodologies has been in the field of biomedical applications, where MSI can routinely reveal the identity and location of a diverse range of biomolecules, including drugs and metabolites, lipids, peptides, and proteins, within biological tissue sections with cellular (and in some cases subcellular) resolution. For example, arguably one of the largest beneficiaries of MSI is the pharmaceutical industry where it allows the uptake and distribution of drugs and metabolites to be analyzed [5]. However, while the field of MSI has seen significant growth in recent years, acquiring quantitative information from MSI data has proven to be difficult and presents arguably its greatest limitation.

Traditional quantitative techniques for biomedical analysis include whole-body autoradiography (WBA) [6, 7] and liquid chromatography-tandem mass spectrometry (LC-MS/MS) [8]. WBA is widely used in the pharmaceutical industry and requires the drug of interest to be labeled with a radioactive isotope. This allows both the distribution and the quantity of the drug to be measured; however, it is not capable of resolving signals from a drug and its metabolites and requires expensive radiolabels. By contrast, LC-MS/MS allows quantitation and identification of multiple components within complex biological mixtures, but analysis is performed on extracts that requires laborious extraction protocols and the loss of spatial information.

Extracting quantitative information from MSI data has proven to be difficult. This is largely due to the high dependency of the MS signal on both the type of analyte and the local composition of the surface. The latter effects are commonly known as “matrix” or “ion suppression” effects and refer to the fact that ion intensities are not simply dependent on the surface concentration of the analyte(s) but also the surrounding chemical environment. Although such effects are invariably present in other quantitative methodologies such

Published in the topical collection *Biomedical Mass Spectrometry* with guest editors Mitsutoshi Setou, Toshimitsu Niwa, and Akira Ishii.

Shane R. Ellis and Anne L. Bruinen contributed equally to this work.

S. R. Ellis · A. L. Bruinen · R. M. A. Heeren (✉)
FOM Institute AMOLF, Science Park 104, 1098 XG Amsterdam, The Netherlands
e-mail: heeren@amolf.nl

Published online: 27 November 2013

as chromatographic approaches [9], the relative simple sample preparation and lack of fractionation in MSI imparts greater influence of these effects on the analysis. Nonetheless, quantitative-MSI (Q-MSI) methodologies are highly sought after and their development is an active area of research. The development of such techniques will allow the simultaneous acquisition of spatial and quantitative data that would be of great benefit, not only to the pharmaceutical industry and drug discovery applications, but for the better understanding of complex biological pathways that are highly dependent on localized molecular composition. However, one must be aware that the requirement of calibration standards for Q-MSI requires a targeted analysis that is only applicable to a small fraction of ions observed in the spectrum.

In this review, we describe the current progress being made to date in the development of Q-MSI methodologies that allow the determination of absolute local concentrations of an analyte per area within a sample. Although outside the scope of this review, it must be emphasized that appropriate sample preparation is critical for any successful MSI/Q-MSI study. The reader is referred to several recent reviews covering this topic [1, 2, 10, 11]. This review aims to bring the reader up to date with the current state-of-the-art in Q-MSI, including its current applications and challenges with a focus on biomedical analysis.

The origin of matrix effects and the requirement of an internal standard

In any quantitative technique, analysis is typically achieved by relating the intensity observed for a particular spectral feature (mass spectrometric or otherwise) to the concentration of the particular analyte(s) giving rise to the spectral feature. In the ideal scenario, the intensity arising from a given analyte would be solely dependent and proportional to its concentration and could, thus, be directly used to provide quantitative information. In practice, however, mass spectrometric signal intensity is not only dependent on analyte concentration but also on ionization efficiency that is strongly influenced both by molecular structure and the surrounding chemical and morphological environments that are sampled simultaneously with the analyte(s). In addition, these relationships are complex and typically do not follow a linear trend. The latter two effects give rise to what are known as "matrix" or "ion suppression effects" that cause ion intensities to become dependent on the environment from which ions are generated. These effects are particularly pertinent for MSI where the high degree of heterogeneity in tissues and cells leads to dramatic changes in the localized environment across the sample. These effects occur coincidently with analyte-specific ionization efficiencies and can lead to dramatic changes in ion yields obtained across a sample, even for analytes present at identical concentrations [12–16]. It is these region-specific effects that invariably make Q-MSI such an analytical challenge. Thus, any quantitative technique must accurately correct for these effects on a pixel-by-pixel basis and allow raw ion intensities to be appropriately calibrated to provide absolute surface concentrations. For these reasons, Q-MSI, like traditional quantitative techniques, requires the use of internal standards (ISs) against which the analyte signal can be calibrated and also to correct for matrix effects. The incorporation and use of ISs represents the most challenging, yet essential, component of a successful Q-MSI study

Desorption/ionization approaches

Although detailed descriptions of the desorption/ionization processes employed for Q-MSI are outside the scope of the review, we have provided brief discussions of each approach described in this review below in order highlight specific issues relating to quantitation that must be considered for each.

Matrix-assisted laser desorption/ionization (MALDI)

MALDI is widely used for MSI of a wide variety of analytes including proteins and peptides [17–21], lipids, pharmaceuticals and metabolites [22–26], direct from a wide range of surfaces and in particular tissue sections [27–29]. MALDI analysis requires the sample surface be coated with matrix, typically a small organic compound, which facilitates analyte extraction and, ultimately, the "soft" ionization of desorbed molecules. A detailed review of the mechanisms of MALDI can be found in references [30, 31]. While appropriate sample preparation is central to any MSI study, the use of a matrix introduces an additional preparation step for MALDI that is not required for other MSI approaches and has important implications for quantitative analysis. [11]. In order for the generated ion images to be representative of the localized concentrations, the matrix must be applied in a homogenous manner that minimizes analyte delocalization. Homogenous matrix application can now be routinely performed with a variety of approaches [32–39]. Crucially, the method of matrix application and the matrix itself have also been shown to influence the types of analytes observed [40] and even the LOD and linear dynamic range of the analysis [41] and, thus, matrix type and application technique requires careful optimization prior to quantitative analysis.

A key consideration for quantitative-MALDI (Q-MALDI-MSI). is that tissue heterogeneity can lead to local changes in analyte extraction efficiency from the tissue into the matrix and crystallization behavior across the surface [10, 42]. Therefore, IS incorporation presents a unique challenge as it must be done in a way such that it mimics as close as possible the extraction, crystallization, and ionization behavior of the targeted analyte(s). Moreover, the matrix can produce a series

of low mass ions that may overlap with the signal from the analyte(s) of interest. Here MS/MS based analyses may present a significant advantage.

Secondary ion mass spectrometry (SIMS)

SIMS analysis involves the bombardment of the sample with a highly focused, accelerated (typically 5–40 keV) ion beam (e.g., Bi^+, Au^+, Cs^+, O_2^+, and C_{60}^+). As the energetic ions impact the surface, they initiate collisional cascades that ultimately lead to the ejection of both neutrals and charged species (so-called secondary ions) from the top few layers (10–50 nm) of the surface [43–45]. As the ion beam can be focused down to ~50 nm, MSI with SIMS can be routinely achieved with sub-micron spatial resolution. The primary disadvantage of SIMS is that the energetic desorption process results in significant fragmentation of desorbed molecules and makes the detection of large intact molecules (such as biomolecules) difficult. This means that SIMS analyses are generally limited to ions with a mass lower than 1000 Da and, as a result, many studies monitor the intensity of characteristic fragments (if present) or simply acquire elemental information. Ion yields in SIMS are dependent on a variety of factors, including concentration and sputtering/ionization yields. Of course, all of these are highly dependent on the local chemical environment. In regards to quantitative data with SIMS, one must be aware that analyte-specific ions may not always be observed and that the generated spectra are only representative of the top few monolayers of the exposed surface and these distributions may not necessarily reflect bulk compositions.

Laser-ablation-inductively coupled plasma-MS (LA-ICP-MS)

In terms of quantitative properties, LA-ICP-MSI typically provides the lowest RSD and highest reproducibility of any MSI approach and routinely provides %RSD values between 5 %–10 % [46], high degrees of linearity, and high sensitivities in the ng/g–μg/g range. The basic operating principle of LA-ICP-MS involves the laser ablation of the sample by a UV laser pulse (typically 213 nm with ablation diameters of ~10–100 μm). The ablated material is then transported by an argon carrier gas into the plasma region where the material is dissociated into its elemental components and ionized to the corresponding cations of which ionization efficiencies are well known. Ions are then transported into the mass spectrometer for analysis. Although elemental imaging is also possible with SIMS, it is likely that the plasma-induced atomization that occurs during LA-ICP-MS affords it a greater elemental ionization yield that is less susceptible to matrix effects. This has been attributed to the separation of the atomization and ionization events in LA-ICP-MS that allows both to be optimized independently [47]. Localized matrix effects may arise from a number of factors, including heterogeneity in the sample, concentration, and the ionization potential of different atoms. These factors can induce selective volatilization, vaporization, ionization, and transport effects [48]. Quantitation strategies for LA-ICP-MSI have been extensively covered in several recent publications [48–52] and will, thus, only be covered briefly here.

Desorption electrospray ionization (DESI)

The recent emergence of ambient ionization techniques, such as DESI [53–55], have provided new approaches to the mass spectrometric analysis of surfaces [54–57]. These techniques allow direct surface analysis outside the confines of the vacuum region of the mass spectrometer with minimal-to-no sample preparation. These capabilities minimize the possibility of sample deformation (e.g., due to rapid dehydration) upon introduction to the vacuum region while allowing analysis of biological samples in (or at least close to) their native state (e.g., whilst still containing native water content). To date, of the ambient imaging techniques, Q-MSI has only been reported with DESI (Q-DESI). DESI analysis is initiated by the bombardment of the sample with a series of highly charged droplets produced by a pneumatically assisted electrospray. As the charged droplets strike the surface, they extract surface-bound analytes that are then released from the surface within scattered secondary droplets. Upon solvent evaporation, these droplets ultimately lead to the formation of intact analyte ions (analogous to ESI) that then enter the mass spectrometer for analysis. Difficulties concerning the acquisition of quantitative data may arise from poor or non-uniform local extraction efficiencies across the tissue and the possible dependence of ion signal on the degree of tissue damage that is dependent on the choice of solvent [58, 59].

Incorporation of internal standards for signal calibration

Ideal internal standard to account for matrix effects

Any quantitative approach requires an internal standard (IS) against which the signal from the analyte(s) is calibrated. In Q-MSI, the IS should both help correct for region-specific matrix effects and allow analyte signal to be converted into absolute surface concentrations upon generation of an appropriate calibration curve. Although there are a variety of approaches for signal normalization in Q-MSI, normalization to the IS signal is by far the most superior technique for both acquisition of quantitative data and ensuring the resulting image provides the most representative reproduction of analyte distribution. This is highlighted in Fig. 1, which provides MALDI-MSI images of imipramine in rat lung tissue with deuterated imipramine doped into the matrix as an IS and applied homogenously

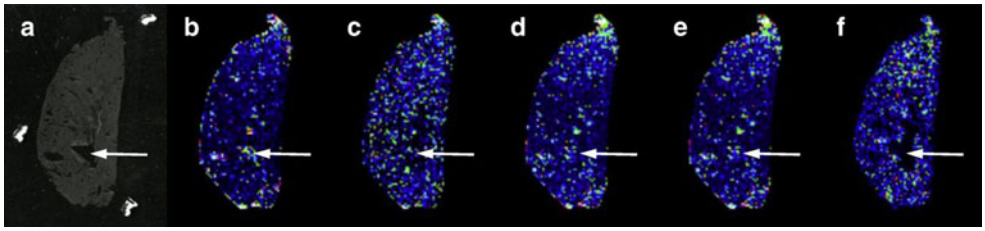

Fig. 1 MALDI-MSI images of imipramine in rat lung tissue acquired following homogenous coverage of tissue with matrix and deuterated imipramine as an internal standard with various normalization strategies. (**a**) Optical image of tissue section. The arrow points to an area where tissue is missing. Ion images are generated with: (**b**) no normalization, (**c**) simple moving median normalization, (**d**) total-ion current (TIC) normalization, (**e**) root-mean-squared normalization, and (**f**) normalization to internal standard signal. All normalization is performed on a pixel-by-pixel basis. Only normalization to internal standard signal is able to account for the lack of analyte signal expected in the region where tissue is missing, and thus provides the most representative image of actual analyte distribution. Image adapted with permission from reference [60]

across the tissue surface [60]. Only pixel-by-pixel normalization of imipramine to the IS signal was able to reproduce the lack of imipramine signal in the region where tissue is missing. All other normalization approaches provided a "false" detection of imipramine in this region. Although there are a variety of means by which ISs are employed in Q-MSI (see below and Table 1), there are several features that define an ideal (and thus suitable) IS. First, the molecular structure of the IS should be as close as possible to that of the analytes targeted for quantitation. This ensures that it is extracted and ionized in a similar manner to the analyte and, thus, corrects for analyte-specific ionization efficiencies. For this reason, stable isotope analogues of the analyte(s) are often chosen if they are available. Second, the IS should be analyzed in an environment identical to or as close as possible to that in which the analytes are present. This helps to ensure that both analyte and IS are exposed to a similar chemical matrix during analysis and, thus, allows correction for region/sample-specific desorption and ionization efficiencies. For this reason, biomedical applications often use cell or tissue homogenates, or even the tissue surface itself, as the matrix into which the IS is incorporated. However, this requirement can be particularly challenging for techniques that require analyte extraction (MALDI and DESI) as the externally applied IS must be applied in a manner that ensures it is also extracted in an analogous manner to the analyte present within the tissue. For example, IS applied on top of the tissue may provide elevated response for the IS relative to the analyte. Alternatively if the IS is present within a cell/tissue homogenate, this may not allow changes in D/I efficiencies that occur across the surface of a single tissue section or cell to be accounted for.

Table 1 Reported calibration approaches for quantitative-MSI of biological material[a]

Technique	Signal calibration method	Analyte/surface	References
SIMS	Relative sensitivity factor (RSF) determined with doped matrix of similar properties (i.e., frozen homogenates)	Elements in cells and tissue	[61–67]
	Relative sensitivity factor (RSF) determined with ion implantation of standards.	Elements in tissue	[68]
DESI	Dilution series on top tissue	Clozapine in rat brain section	[69]
MALDI	Dilution series deposited under control tissue; matrix applied after	Cocaine and acetyl-l-carnitine in brain tissue sections	[70–72]
	Dilution series on top of control tissue; matrix applied after	Tiotropium in rat lung sections, digested proteins in coronal rat brain sections	[73, 74]
	Calculation of tissue-specific extinction coefficient to account for on-tissue suppression effects	Propranolol and olanzapine in whole body sections of mice.	[75]
	Dilution series on top of control tissue with labeled IS pre-mixed with matrix.	Imipramine, tiotropium, and Substance P in tissue sections	[60]
	Normalization of ion counts per pixel by quantitation with LC-MS/MS of tissue homogenate	Olanzapine in rat liver sections	[76]
	Dilution series of analyte prepared within a tissue homogenate of rat liver	Lapatinib and nevirapine in rat liver, dog liver and xenograft mouse tumor	[77]
LA-ICP-MS	Calibration with suitable certified reference materials (CRM)	Elements in tissues	[78–80]
	Calibration in matrix matched standard or a matrix with similar properties.	Elements and nanoparticles in cells and tissues.	[46, 51, 81–93]
	Online addition of standards with simultaneous sample ablation	Elements in tissues	[81, 90, 94–97]
	Isotope dilution	Elements in tissues	[98, 99]

[a] This table is not intended as a complete summary of all approaches employed for Q-MSI of biological samples, but rather serves to highlight a variety of different methods that may be used

Matrix-matched standards with homogenates

Matrix-matched standards, commonly used for quantitative LA-ICP-MSI (Q-LA-ICP-MSI) and SIMS (Q-SIMS-MSI) studies, are approaches that incorporate IS within a homogenized matrix that has similar properties to that of the sample. This ensures that matrix effects within the sample are closely mimicked and tissue/cell-specific matrix effects are corrected for. In terms of biomedical studies, this is widely (but not always) achieved using cell or tissue homogenates of the same origin as the sample. However, for whole body samples, this can necessitate time-consuming sample preparation steps as homogenates must be prepared from each tissue type of interest. In addition, it must be noted that by their nature, tissue homogenates may not accurately account for changes in ion suppression effects that arise from heterogeneity across a tissue or cell surface that is commonly encountered in MSI.

The use of matrix-matched standards has been widely applied to Q-SIMS-MSI through the use of relative sensitivity factors (RSFs) [65]. RSFs relate the ion intensity ratio of the analyte(s) of interest to a homogenously distributed component present in the sample (commonly ^{12}C is used for organic material). Thus, if the RSF is known, by measuring the ratio of the ion of interest to the matrix component the absolute localized concentration of the analyte within the analyzed area may be calculated. The RSF is typically determined using doped cell or tissue homogenates, although controlled ion implantation has also been employed [14, 68] (Table 1). In an early study, Ausserer et al. performed Q-SIMS-MSI to quantify the amounts of boron, calcium, magnesium, potassium, and sodium in cultured cells [65]. To calculate RSFs, frozen cell homogenates spiked with $Na_2B_{12}H_{11}SH$ were analyzed by both SIMS and inductively coupled plasma-atomic absorption spectroscopy. The latter technique was used to relate the measured SIMS intensities to absolute concentration. Determined RSFs were then used to quantify a range of elements ($mmol/kg_{dry\ weight}$) within the nuclear, perinuclear, and cytoplasmic regions of single fibroblast cells. RSFs have been applied for the Q-SIMS analysis of a range of biological samples, including frozen-hydrated samples [62], aluminium deposits in brain tissue [64], and a variety of elements within single cells [61, 63, 66, 100, 101]. For example, the quantity of boron uptake in tumor cells was analyzed in the context of boron neutron capture therapy using the RSF approach [63, 67]. In the study by Smith et al. rats were dosed with *p*-boronphenylalanine (BPA) and analyzed by Q-SIMS [63]. The distribution and uptake of BPA was determined by monitoring the ratio of ^{10}B to ^{12}C signals and this was related to absolute boron content (calculated in $\mu g/g_{tissue}$) through the known RSF. This Q-SIMS-MSI analysis revealed elevated level of boron uptake in the main tumor mass relative to contiguous normal brain tissue and, importantly, levels above 15–30 $\mu g/g_{tissue}$ that are essential for the therapeutic process were observed.

Conventional calibration curves generated from standards in a suitable environment have also been used for Q-SIMS-MSI [102–104]. Using this technique, Strick et al. [102] quantified a variety of elements within individual fibroblast cellular compartments and single chromosomes. First, a calibration curve was generated using doped agarose and revealed a 10 nM sensitivity for Ca^{2+} and a 100 nM sensitivity for Mg^{2+}. The average concentration in a diploid set of chromosomes was determined to be in the range of 20–32 mM for Ca^{+} and 12–22 mM for Mg^{2+}. Furthermore, the SIMS-MSI analysis revealed a Ca^{2+}:Mg^{2+} ratio of 3:1 on the chromatoid axis, providing evidence that that Ca^{2+} is enriched in AT-rich axes.

Although a variety of quantitative approaches for Q-LA-ICP-MSI have been demonstrated (Table 1), including online addition employing a nebulizing sprayer, isotope dilution, doped polymer films, and inkjet printing of standards [48, 49, 84, 91, 98, 99, 105, 106], the use of matrix-matched standards for calibration has been the most popular approach. The use of matrix-matched IS for Q-LA-ICP-MSI was first demonstrated by Becker et al. [90] for the imaging of a variety of elements in human brain tissue. In this approach, a tissue homogenate doped with suitable standards is used to closely mimic the ablation and ionization of endogenous analyte from the sample. The doped homogenate is frozen, sliced, and analyzed to generate a calibration curve that is then applied to the sample of interest. This approach allowed Q-MSI of elements including zinc, copper, thorium, and uranium at sub-ppm levels in the human brain. Representative data acquired for zinc and copper are provided in Fig. 2. The highest zinc concentration was found in the hilus and lucidum regions of the hippocampus, whereas copper was observed to be enriched overall in the hippocampus. By contrast, thorium and uranium were present at lower levels and were homogenously distributed. Nanoparticle doped nitrocellulose membranes have also been employed as a cell-mimicking calibration approach to allow for quantitation of gold and silver nanoparticle uptake in single fibroblast cells [89]. Cultured cells were incubated with gold and silver nanoparticles and analyzed by LA-ICP-MSI (laser spot size of 4–8 μm) using an oversampling approach to provide sufficient spatial resolution. LOD and LOQs for silver nanoparticles with a 50 nm average diameter were 20 and 60 particles, respectively. In agreement with the smaller particle size, detection of gold nanoparticles with an average diameter of 25 nm could be achieved with an LOD of 190 particles and LOQ of 550 particles. Cells incubated with silver nanoparticles at a concentration of 0.2 and 2 pM for 24 h were found to contain on average 380 and 2500 particles per cell, respectively. However, incubation at 20 pM revealed toxic levels of 15,000–57,000 particles present in the cell. The ability to quantify nanoparticles in single cells highlights the potential for Q-LA-ICP-

MSI in areas such as nanotoxicity and even the characterization of nanoparticle-based drug delivery systems [107].

The usefulness of matrix-matched standards in Q-LA-ICP-MSI has led to a variety of certified reference materials (CRMs) becoming commercially available for use as standards to aid in LA-ICP-MSI calibration [48, 52]. For example, CRM based on bone meal has been used for Q-LA-ICP-MSI of trace elements in human teeth, and distinct distributions between enamel, prenatal dentine, postnatal dentine, and secondary dentine could be observed [92] (Fig. 2c). In another study, bovine liver matrix was employed for the analysis of trace metals in liver disorder [93]. To ensure equivalent plume conditions, it is essential that the calibration sample composition (such as water content) matches as close as possible the sample to be analyzed. To ensure close matching, for many applications home-made standard samples must be prepared from for example tissue homogenates, if appropriate CRMs are not available.

An alternative approach for signal calibration in Q-LA-ICP-MS related to matrix-matched standards is the use of online addition. In this approach, a series of solutions doped with known concentrations of elements is nebulized concurrently with laser ablation of an unspiked tissue homogenate section to produce the calibration curve to which signal acquired from the sample is calibrated against. The simultaneous ablation of the tissue homogenate ensures the chemical environment of the sample introduced into the plasma closely resembles that of the tissue samples to be analyzed and, thus, any matrix effects are taken into account. This approach has been used by Pozebon et al. for the Q-MSI of 29 elements in brain sections [94]. A similar approach has also been used for the spatially resolved quantitative analysis of elements in hair [97], steel, and glass [108]. One possible disadvantage of this approach is the dilution of the endogenous analytes that can affect the LOD [95].

Recently, the matrix-matched standards approach has been extended to the analysis of drug distributions by Q-MALDI-MSI [77]. In this study, a mimetic tissue model based on dosed tissue homogenates was developed to allow for signal calibration and absolute quantification with MALDI-MSI. Tissue homogenates were prepared from rat liver tissue and dosed with known concentrations of the drugs lapatinib and nevirapine and then frozen in a polymer support mould. Importantly, to ensure similar analyte extraction and matrix crystallization between the homogenates and tissue, homogenates were shown to be prepared with a similar density and distribution of cell nuclei as the original tissue. Thin sections of the homogenates and tissues were then prepared at the same thickness and mounted next to each other on a glass slide. Calibration curves allowing for endogenous analyte signal calibration were generated by analyzing homogenate sections containing a known range of dosed analyte and averaging the signal intensity acquired across the homogenate surface. Calibration curves generated for lapatinib revealed R^2 values >0.99 and linearity over 3 orders of magnitude range in concentration (62–61,600 ng/g). In addition, high reproducibility of the ion signal acquired from the homogenates was observed with RSDs between 1.94 % and 11.88 % reported across the concentration range. Finally, by calibrating analyte signal from dosed tissues against the generated calibration curves, determination of the absolute concentration (averaged across the tissue surface) of dosed nevirapine (in rat liver) and lapatinib (in dog liver and a mouse xenograft tumor tissue) was possible. In all cases, absolute Q-MALDI-MSI quantities

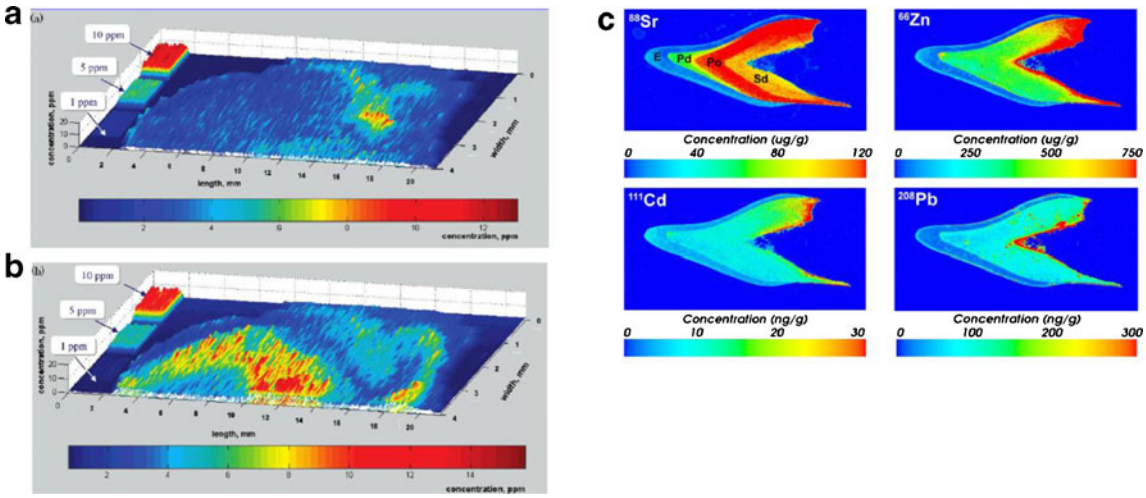

Fig. 2 Q-LA-ICP-MS images of zinc (**a**) and copper (**b**) in human hippocampus tissue section. Calibration was performed using doped tissue homogenates. Calibration spots are shown on the left of the corresponding images for homogenate doped with 1, 5, and 10 ppm of the corresponding element. Image taken with permission from reference [90]. (**c**) Q-LA-ICP-MS of four trace elements within a human tooth. Calibration was achieved by analysis of a standard reference material (NIST SRM 1486 bone meal). Image taken with permission from reference [92]

were within 10 % of the concentrations acquired by LC-MS/MS analysis of serial section from the tissue. These results demonstrate the ability of the rat liver homogenate to provide a suitable matrix for quantitation in dog liver and mouse xenograft tumor tissue, thus suggesting that it is not always essential for homogenates to be prepared from the same tissue to be analyzed. For example, the concentration of lapatinib in dog liver was determined to be 110,000 ng/g_{tissue} by Q-MALDI-MSI compared with a value of 120,000 ng/g_{tissue} obtained by LC-MS/MS. This close agreement verifies the accuracy of the approach, at least for the determination of average concentrations across a tissue surface and the ability of the tissue homogenates to closely mimic the extraction, crystallization, and ionization conditions encountered during tissue analysis by MALDI.

Dilution series of IS on or below tissue section

The use of dilution series spotted on top of or below tissue sections for signal calibration has been widely explored in quantitative MALDI-MSI (Q-MALDI-MSI) studies where intact biomolecules are routinely observed from tissue. In these approaches, the idea of preparing and analyzing the IS dilutions series in contact with the tissue is thought to replicate tissue-specific matrix effects. However, while this may partly be the case, it is very difficult to exactly replicate the extraction, desorption, and ionization conditions encountered for an analyte initially present within the tissue using an externally applied IS. Nonetheless, the studies highlighted below show that good agreement with established quantitative approaches such as LC-MS/MS can be achieved and suggest that these effects can be closely (although not exactly) replicated.

One of the most common approaches for this methodology has been to prepare the dilution series on top of the tissue section. The ion signal from the dilution series is used to produce a calibration curve against which the analyte signal is calibrated. In one successful study, Q-MALDI-MSI was employed to investigate the in vivo uptake and retention of inhaled triotropium, a drug used in the management of chronic obstructive pulmonary disease, in rat lung tissue [73]. To allow quantitation, serial dilutions of triotropium were spotted onto an undosed tissue and calibration curves were generated using the intensity of the characteristic tiotropium ions (or fragments) in both MS and MS/MS mode. Both calibration curves provided good linearity with R^2 values of 0.995 for deposited amounts of 80 fmol–5 pmol of tiotropium standard in MS/MS mode and R^2 value of 0.983 for 80 fmol–2.6 pmol in MS mode. Regions of interest (20–25 pixels with pixel size of 175–200 μm) for areas observed by MSI to contain low, medium, and high counts for triotropium in dosed tissue were analyzed and the abundances present on the surface inferred from the calibration curve. This analysis provided surface concentrations of ~0.2–1.30 pmol per 20–25 pixel region across the tissue area and correlated well with absolute values determined by LC-MS/MS of tissue homogenates. In a more recent study, an on-tissue deuterated peptide was used for the quantitative MSI of myelin basic protein (MBP) in rat brain [74]. In this study, an on-tissue trypsin digestion was performed to convert intact proteins into a range of peptides characteristic of the intact proteins. Crucially, the on-tissue digestion ensured that the spatial distribution of tryptic peptides was indicative of the spatial distribution of their protein precursor. Quantitative analysis was carried out by homogenously spraying a deuterated analogue of a MBP-specific peptide over the tissue section using a commercial automatic spray deposition device. The surface concentration of sprayed IS was calculated by depositing a dilution series of the analogous unlabeled peptide standard over the deuterated IS layer sprayed onto a blank slide. Using the known concentrations of unlabeled peptide on the surface and the nominal ablation spot diameter of 50 μm per pixel, the surface concentration of the deuterated IS was calculated to be 93± 0.1 amol/ablation area. MSI was then performed using multiple reaction monitoring (MRM) transitions specific for the endogenous and labeled peptides. Calibration of the on-tissue signal for the endogenous MBP-specific peptide to the labeled peptide allowed quantitation of the endogenous peptide and, hence, MBP. Concentrations of MBP in rat brain were calculated to be 0.001–0.071 amol.μm^{-3}, although no verification of these values by an alternative approach was provided. Additionally, it is likely that the extraction efficiency for endogenous compounds likely differs from that of an IS applied on top of the tissue, and this could lead to errors in the concentration of endogenous compounds within the tissue volume.

As an alternative to preparing IS on top of tissue the Yost group has explored the deposition of IS beneath the tissue surface. As the IS must be extracted through the tissue volume into the matrix layer on top of the tissue, it has been proposed that this method of IS preparation is able to more accurately reproduce the extraction and crystallization of endogenous analytes within the matrix layer. Pirman et al. demonstrated the use of this technique to correct for tissue and region-specific ion suppression effects [71]. For example, ion suppression effects occurring when analyzing different regions of a piglet brain tissue could be compensated for by normalizing to the IS signal. In this analysis, calibration spots of acetyl-$_L$-carnitine (AC) were deposited on a glass slide and were then covered homogenously with the deuterated IS prior to mounting of the tissue section and matrix application. Figure 3a shows the MS-image of protonated AC. Both the calibration spots and endogenous AC are observed. At first glance, it appears that there is significantly less AC in the white matter compared with grey matter. However, analysis of the protonated AC-d_3 also reveals this trend (Fig. 3b), suggesting that lower extraction/ionization efficiencies in white matter may be the cause of this observation. Figure 3c shows the ratio image

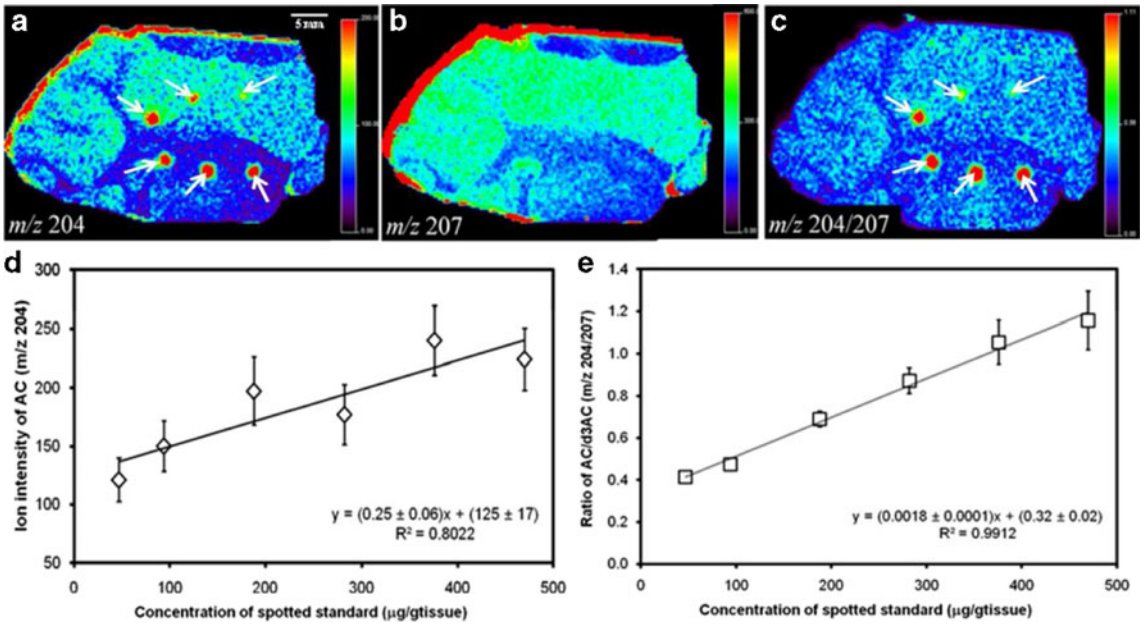

Fig. 3 MALDI-MSI of endogenous acetyl-l-carnitine (AC) in a piglet brain tissue section. (**a**) Ion distribution image of the $[M + H]^+$ ion of AC at *m/z* 204, which reveals a clear differentiation between white and grey matter. (**b**) Ion distribution image of homogeneously applied AC-d_3 internal standard ($[M + H]^+$ ion at *m/z* 207). This image also reveals differentiation of white and grey matter that arises from tissue-specific ion suppression effects. (**c**) Ratio images of *m/z* 204/207 on a tissue section on which a dilution series of AC was initially deposited below the tissue (50–460 µg/g_{tissue}) and covered homogenously with AC-d_3. The dilution series was used to generate the calibration curves shown in (**d**) and (**e**). d Shows the calibration curve generated using only the $[M + H]^+$ ion of AC. e Calibration curve generated by using the ion intensity ratio of *m/z* 204/207 (AC/AC-d_3). The latter normalization procedure reveals a significantly greater linearity (greater R^2 value) in the calibration curve. Image taken with permission from reference [71]

of *m/z* 204/207 (AC/AC-d_3) where pixel-to-pixel normalization has been performed. Although this image also suggests there is more AC in the white matter, the difference between white and grey matter is noticeably less following normalization. This image, by accounting for spot-to-spot signal variation, likely provides a more accurate representation of the AC distribution (although no external verification of the AC distribution was provided) and, thus, highlights the need for an IS in quantitative MSI. Normalization of the dilution series to an internal standard also results in a more linear calibration curve.

This approach has also been extended to allow the absolute Q-MSI of acetyl-$_L$-carnitine [70] and cocaine [72] from piglet and human brain tissue, respectively. In the latter study, cocaine in brain tissue was quantified utilizing an analogous calibration procedure using cocaine-d_3 as the IS with MS/MS image acquisition. Signal calibration was performed using standard addition by application of a cocaine dilution series and a homogenous layer of IS beneath the section. Q-MSI performed with quadrupole-time-of-flight (Q-ToF) instrumentation provided cocaine concentrations of 240±100 ng/g_{tissue} and 400±50 ng/g_{tissue}. Surprisingly, a similar analysis performed with an ion trap instrument reported a much higher cocaine concentration with larger uncertainty within each measurement (880±300 ng/g_{tissue}). This was attributed to the less powerful nitrogen laser used for the ion trap measurements and the fact that only several laser shots were accumulated in the ion trap for each raster spot to avoid space charge effects. As a result only a small percentage of the tissue surface was ablated, leaving behind much analyte and IS. The Q-ToF system used a more powerful solid-state laser and acquired 200 laser shots per raster position. This resulted in near complete ablation of each raster spot and, thus, sampling of all material present at each raster spot. This not only improves signal and, thus, provides better statistics but also helps compensate for uneven extraction of IS through the tissue to the surface that may arise when the IS is placed beneath the tissue. It would be expected that the IS concentration would be lowest at the tissue surface, and this can result in elevated analyte:IS ratios. An additional source of error in these measurements may lie in the determination of the concentration of cocaine and IS initially present beneath the tissue [72]. Lateral diffusion through the tissue during extraction may spread out standards across a larger surface (lower concentration per area) then the area of the initial droplet, and this would be expected to vary with tissue thickness and mobility of deposited standards through the tissue. Nonetheless, cocaine quantities measured by Q-MSI were compared with those obtained following LC-MS/MS analysis of extracts. As expected, the more established LC-MS/MS approach provided much higher precision and linearity (RSD 5.5 %–6 % and R^2 values >0.99). However, within the error of the experiment, Q-ToF values compared favorably with LC-MS/MS analyses, providing evidence that IS applied under the tissue, in addition to MS/MS acquisitions and complete ablation of

each raster position, allows for absolute quantitative analysis using MSI.

The doping of IS into the MALDI matrix has also been reported by Källback et al. for the Q-MALDI-MSI of several drugs (imipramine and triotropium) and the peptide Substance P [60]. Deuterated ISs were doped into the matrix solution and then applied to the tissue section using an automated spray deposition device. Drug calibration curves were generated by spotting serial dilutions of analyte standard onto control tissue sections followed by simultaneous matrix and IS application. Peptide quantitation was achieved by deposition of dilution series of Substance P onto the cerebral cortex (a region known to contain minimal endogenous Substance P) for calibration followed by matrix and IS application. Signal for the analytes of interest within regions of interest (ROI) were then compared with the appropriate calibration curve and allowed the analyte concentration per area or weight of tissue within the ROI to be calculated. Applying this technique to endogenous Substance P within different mouse brain structures revealed the highest concentrations in the substantia innominata (22 fmol/mg) and substantia nigra (42 fmol/mg). The quantitative MSI results were compared with previous results obtained by radioimmunoassay [109]. For example, the quantitative MSI approach provided Substance P concentrations in the caudoputamen of 13 fmol/mg compared with 21 fmol/mg measured with the radioimmunoassay. Although the results are in reasonable agreement, possible sources of the lower values obtained with MSI are incomplete extraction and incorporation of Substance P into the matrix crystals and the IS that is pre-mixed with matrix prior to deposition. The latter effect will likely lead to different incorporation of IS and endogenous molecules into the matrix crystals. Furthermore, this approach may not effectively account for changes in ion suppression effects across the tissue surface as the calibration curve was acquired from standards deposited onto different tissue regions to where the endogenous peptide is located.

On-tissue dilutions series have also been employed to provide the first report of Q-MSI using DESI (Q-DESI) (Fig. 4) [69]. Here, a calibration curve was first generated by pipetting a dilution series of clozapine in the presence of an isotopically labeled clozapine onto undosed rat brain section. The calibration curve revealed a dynamic range over 3-orders of magnitude and returned an error of only 3 %–5 % when analyzing quality control samples of known concentration. Using this calibration curve, Q-MSI was then performed by pipetting known amounts of IS onto brain regions where clozapine was known to be located to allow calibration of the average ion signal acquired from the region of interest. Representative ion images of clozapine obtained from two rats are provided in Fig. 4. By comparing the ion intensity of clozapine to the IS in pixels where both were detected, the absolute amount of clozapine per area of tissue could be calculated. The accuracy of the method was verified by analysis of adjacent sections by LC-MS/MS, which revealed only ~9 % difference compared with quantities determined by Q-DESI-MSI (Fig. 4f). Additionally, the RSD of the quantitative method across five sections each from two rats (11 %–17 %) was comparable to that acquired by LC-MS/MS (11 %–13 %). However, this approach relied on the assumption that clozapine was homogeneously distributed within the region of interest and, as noted by the authors, if a heterogeneous distribution is present, the calibration procedure will need to be performed separately on each region where analyte is detected. Finally, use of a radiolabeled IS allowed the extraction efficiency of DESI to be evaluated, and it was revealed that only 15 %–20 % of the IS was extracted from the tissue during a single DESI-MSI analysis. In terms of Q-MSI, this effect introduces an error in knowing exactly how much material is analyzed and is likely to vary with different analytes and substrates. Moreover, it may likely result in different extraction efficiencies for on-tissue IS and endogenous compounds during DESI that may lead to errors in calculated concentrations.

Q-MSI in the absence of internal standards

Although ISs are thought to be essential for any quantitative analysis, several recent studies have reported Q-MALDI-MSI without the use of an IS. Here, Q-MSI is performed either by finding a correction factor for matrix effects or employing an alternative quantitative technique against which MSI data can be normalized. These approaches and their advantages/disadvantages are discussed briefly below.

The approach reported by Hamm et al. [75] involves the calculation of an analyte and tissue-specific normalization factor termed the "tissue extinction coefficient" (TEC). To calculate the TEC for a specific analyte/tissue combination, both a glass slide and tissue section are homogenously sprayed with an analyte/matrix mixture. The ratio of analyte intensity from a specific control tissue region to that acquired from the glass slide gives the TEC value. By analyzing a whole-body rat section in a single analysis, the analyte-specific TEC values for different tissue regions can be calculated and can be used to account for signal variation arising from tissue-specific ionization suppression effects; thus, in some ways, this approach is similar to the RSFs employed from SIMS (see above). As the TEC effectively provides a measure of the extent of tissue-specific ion suppression, TEC values are calculated for each different tissue/analyte combination of interest. Although not always true, tissue regions assigned a TEC value are assumed to be homogenous. As shown in Fig. 5, determination of the TEC values for propranolol acquired from a variety of rat organs revealed TEC values were highest from the stomach (indicating less ion suppression) and lowest from the brain and liver (more ion suppression). However, the TEC values of the kidney and brain had

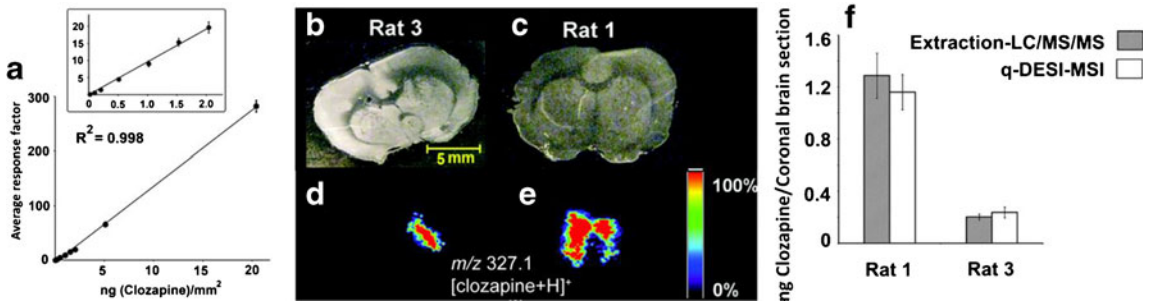

Fig. 4 (**a**) Calibration curve for clozapine standards micropipetted onto a coronal rat brain section and analysed with DESI-MS. Average response factors were calculated for all scans in all rows of data that clozapine and IS were both detected with four replicates for each concentration. (**b**) and (**c**) Optical images of two coronal rat brain sections prepared following clozapine dosage (2.5 mg/kg^{-1}, 45 min postdose). (**d**) and (**e**) Corresponding DESI-MSI images of the clozapine $[M + H]^+$ ion at *m/z* 327.1. Quantitation was achieved based on the calibration curve generated by deposition of a dilution series of clozapine on an untreated tissue section. (**f**) Comparison of Q-DESI-MSI and LC-MS/MS of adjacent tissue sections obtained from five measurements of five different sections. Error bars represent the corresponding standard deviation. Q-DESI-MSI quantities are within 9 % to those acquired by LC-MS/MS. Image adapted with permission from reference [69]

the highest variation that is likely due to the large degree of tissue heterogeneity, which will influence the precision of the analysis. Once the TEC values are known, a calibration curve is produced by Q-MSI analysis of a dilution series of the analyte of interest on the glass slide adjacent to the tissue. Using the TEC value and calculated tissue density, endogenous ion signal acquired from a particular tissue region or ROI can then be calibrated to provide the analyte concentration per unit area or weight of tissue section. Advantages of this approach include the ability to generate Q-MSI data from different tissue regions (such as that encountered in a whole body imaging experiment) in a single acquisition (once the TEC values are known) and that a deuterated internal standard is not required, thus making it well suited for early drug discovery studies. Furthermore, the approach may be applied to any desorption/ionization technique. However, as the TEC value is based on the signal acquired using analyte spotted onto the tissue surface, it is important to note incomplete (and tissue-specific) analyte extraction into matrix crystals may not be completely taken into account for endogenous analyte(s) initially present within the tissue volume. Nonetheless, very promising results for the quantitative-MSI analysis of both propranolol in whole body rat sections and olanzapine in rat kidney were obtained with RSDs less than 7.8 % compared with corresponding data acquired with an established Q-WBA approach. For example, quantitation of propranolol could be achieved with an LOD and LOQ of 6 and 18 fmol/mm^2,

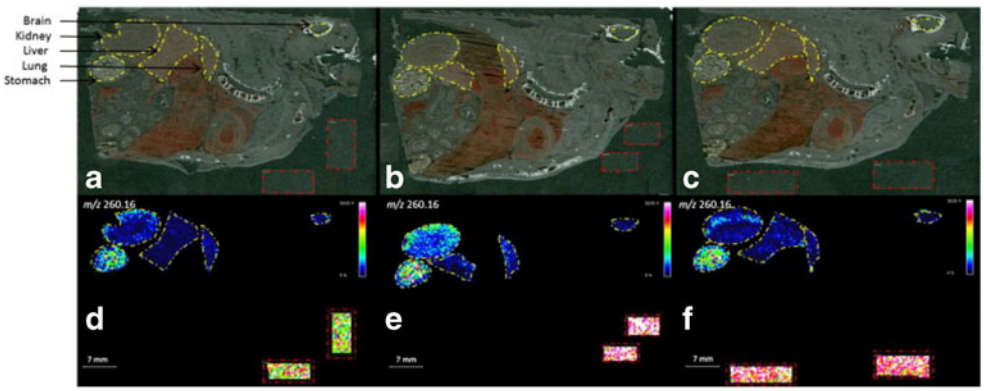

Fig. 5 Optical images of whole body rat section prior to homogenous coverage with a mixture of propranolol (*m/z* 260) and MALDI matrix. Sections and adjacent glass slide were covered with (**a**) 0.5 pmol/μL, (**b**) 5 pmol/μL, and (**c**) 10 pmol/μL of propranolol. (**d**)–(**f**) Corresponding MALDI-MSI images of protonated propranolol at *m/z* 260 acquired from glass slide and tissue covered with (**d**) 0.5 pmol/μL, (**e**) 5 pmol/μL, and (**f**) 10 pmol/μL of propranolol. (**g**) Calculated tissue-extinction coefficients from various organs/tissues within the above sections. Image adapted with permission from reference [75]

g

Organ/Tissue	Standard concentration (pmol/μL)	TEC Values 0.5	5	10	Mean TEC Value	RSD (%)
	Brain	0.098	0.048	0.06	**0.07**	37.9%
	Stomach	0.392	0.354	0.39	**0.38**	5.8%
	Kidney	0.147	0.174	0.09	**0.14**	31.8%
	Liver	0.067	0.049	0.06	**0.06**	15.9%
	Lung	0.104	0.082	0.07	**0.08**	23.0%

respectively. The drug was found to be localized inhomogenously throughout the whole body section, with elevated levels of 5.6, 17.7 and 10.8 $\mu g/g_{tissue}$ calculated from the kidney, lung, and brain, respectively.

In the second approach, integrated MALDI-MS/MS analyte ion counts acquired across tissue section are normalized to quantitative data acquired following extraction and LC-MS/MS analysis of adjacent tissue sections [76]. This allows the average quantity of analyte that contributes to each MS/MS ion count unit (as recorded by the instrument software) to be determined, which can then be related to tissue surface concentration. This technique has been applied to rat liver tissue obtained from rats dosed with varied amounts of clozapine. Normalization of ion counts to LC-MS/MS data yielded a conversion factor of 6.3±0.23 fg clozapine/ion count. The primary advantage of this approach is that an IS is not required; however, time-consuming extraction and LC procedures are required for each analyte/tissue combination to be analyzed and, as this is an average value, the accuracy of this per-pixel quantity may not reflect localized concentrations. In addition, it may also be affected by factors such as the possibility of different extraction/ionization efficiency across the tissue and also changes in instrument performance during the acquisition (e.g., source contamination) that arise as a result of not being able to normalize to an IS.

Validation of Q-MSI data

Finally, despite the significant progress that has been made in the field of Q-MSI (see above), the true accuracy and suitability of any quantitative approach can only be determined once data has been validated. However, validation of Q-MSI data remains a significant technical challenge that must be addressed. This requires the Q-MSI data to be directly compared with data acquired using an independent quantitative methodology such as LC-MS/MS and Q-WBA on the same sample. In Q-MSI studies, where this has been performed, good agreement with surface concentrations acquired by Q-MSI and other quantitative approaches has been reported [60, 70, 72, 73, 75]. However, in most cases Q-MSI was performed by averaging the analyte:IS signal ratio either across the whole tissue section or particular tissue regions. Therefore, a bulk measurement (i.e., LC-MS/MS performed following homogenization and extraction from tissue) is often used to validate another "bulk" measurement acquired across the tissue surface by averaging ion counts across multiple pixels during Q-MSI analysis. While this can verify if the Q-MSI protocol employed allows accurate determinations of *average* surface concentration across a particular area, it negates the pixel-by-pixel positional information that is argued to be one of the primary advantages of Q-MSI over approaches relying on homogenization and extraction. Therefore, the question must be asked as to how much quantitative information (if any) can confidently be drawn from the analyte signal acquired from two adjacent pixels. This requires determinations to be made for regions spaced by 200 μm or less (i.e., the spatial resolution of the image), and validation on this size poses a significant technical challenge with current technology and, furthermore, as the spatial resolution of MSI is constantly being improved, this question is becoming increasingly significant. For example, validation of cellular Q-SIMS-MSI data is rarely performed. Biologically, validation on this size scale becomes essential if one wishes to make quantitative conclusions regarding the concentration of a particular substance in adjacent cells. However, on these size scales (<200 μm), heterogeneity on the sample surface, IS coverage and, in the case of MALDI, matrix crystallization, will invariably be present and makes validation extremely difficult at the present time. One possible solution to validating Q-MSI data on the scales is the use of laser microdissection to cut out regions of tissue composing only a few cells and then performing an extraction-based quantitative analysis on this region [110]. However, full validation of an entire tissue surface using this approach will require many laborious dissections and extractions and, thus, may not be feasible in many cases. Alternatively, liquid microextraction techniques, such as liquid extraction surface analysis (LESA) [111] and the liquid microjunction surface sampling probe (LMJ-SSP) [112], which allow greater control over localized analyte extraction, may provide another method by which localized tissue concentrations can be supported and validated. However, currently the spatial resolution of these techniques (typically ~0.6–2 mm) is less than that achievable with MSI, and this may limit their ability to validate localized concentrations on the order of the pixel size of the MSI experiment.

Summary and future outlook

Although absolute Q-MSI still remains a significant analytical challenge, the studies discussed in this paper highlight the significant progress that is being made in the field. These advances are largely related to the development and optimization of IS-based signal calibration protocols that allow the correlation of ion intensities to an absolute surface concentration (Table 1). It must be noted, however, that as Q-MSI requires the use of internal standards for calibration of analyte signal, an applied method is only suitable for a specific analyte/sample combination and, thus, unlike conventional MSI that allows the imaging of hundreds of molecules in a single, untargeted analysis, Q-MSI necessitates a targeted analysis where only one or several molecules can be analyzed. Nonetheless, where direct comparisons are possible, Q-MSI values are typically within 20 % of those obtained with more established quantitative techniques, an acceptable value for a

range of applications such as early drug discovery. However, as mentioned above, Q-MSI studies typically report an average concentration over a particular tissue region, what is effectively a bulk measurement. The validation and ability to make accurate quantitative judgements on a pixel-by-pixel basis currently represents a significant challenge for the field that must be addressed.

Future advancements in Q-MSI may arise via its coupling with ion mobility, which has the potential to allow quantitation of isomeric species that otherwise constitute unresolved MS signals [113, 114], and also by developing Q-MSI strategies that may be implemented with the wide range of ambient ionization techniques that are becoming increasingly prevalent and offer several key advantages over traditional, vacuum-based mass spectrometric techniques [54, 55, 115]. In particular, these approaches can be applied to the direct analysis of biological samples closer to their native state and, with appropriate sample preparation allowing for the incorporation of ISs, could also potentially find success for Q-MSI applications.

A limitation of Q-MSI approaches is the need for time-consuming data analysis and calibration; however, recently several software packages designed to accelerate these steps have been reported [60, 116] and should increase the accessibility of Q-MSI to many laboratories. Finally, despite the highly promising recent advances in the field, Q-MSI methods are still far from robust and the true applicability of these methods will only become clear with time as they are validated and are applied to an increasing number of analyte/surface combinations.

Acknowledgments Part of this research is supported by the Dutch Technology Foundation STW, which is the Applied Science Division of NWO, and the Technology Programme of the Ministry of Economic Affairs, Project OTP 11956. This work is part of the research program of the Stichting voor Fundamenteel Onderzoek der Materie (FOM), which is financially supported by the Nederlandse organisatie voor Wetenschappelijk Onderzoek (NWO).

References

1. Passarelli MK, Winograd N (2011) Lipid imaging with time-of-flight secondary ion mass spectrometry (ToF-SIMS). Biochim Biophys Acta Mol Cell Biol Lipids 1811(11):976–990. doi:10.1016/j.bbalip.2011.05.007
2. Chughtai K, Heeren RMA (2010) Mass spectrometric imaging for biomedical tissue analysis. Chem Rev 110(5):3237–3277. doi:10.1021/cr100012c
3. Norris JL, Caprioli RM (2013) Analysis of tissue specimens by matrix-assisted laser desorption/ionization imaging mass spectrometry in biological and clinical research. Chem Rev 113 (4):2309-2342. doi:10.1021/cr3004295
4. McDonnell LA, Heeren RMA (2007) Imaging mass spectrometry. Mass Spectrom Rev 26(4):606–643. doi:10.1002/mas.20124
5. Prideaux B, Stoeckli M (2012) Mass spectrometry imaging for drug distribution studies. J Proteome 75(16):4999–5013. doi:10.1016/j.jprot.2012.07.028
6. Solon E, Schweitzer A, Stoeckli M, Prideaux B (2010) Autoradiography, MALDI-MS, and SIMS-MS imaging in pharmaceutical discovery and development. AAPS J 12(1):11–26. doi:10.1208/s12248-009-9158-4
7. Solon EG, Kraus L (2001) Quantitative whole-body autoradiography in the pharmaceutical industry: survey results on study design, methods, and regulatory compliance. J Pharmacol Toxicol Methods 46(2):73–81. doi:10.1016/S1056-8719(02)00161-2
8. Lee MS, Kerns EH (1999) LC/MS applications in drug development. Mass Spectrom Rev 18(3/4):187–279. doi:10.1002/(SICI)1098-2787(1999)18:3/4<187::AID-MAS2>3.0.CO;2-K
9. Taylor PJ (2005) Matrix effects: the achilles heel of quantitative high-performance liquid chromatography-electrospray-tandem mass spectrometry. Clin Biochem 38(4):328–334. doi:10.1016/j.clinbiochem.2004.11.007
10. Heeren RMA, Kükrer-Kaletaş B, Taban IM, MacAleese L, McDonnell LA (2008) Quality of surface: the influence of sample preparation on MS-based biomolecular tissue imaging with MALDI-MS and (ME-)SIMS. Appl Surf Sci 255(4):1289–1297. doi:10.1016/j.apsusc.2008.05.243
11. Goodwin RJA (2012) Sample preparation for mass spectrometry imaging: small mistakes can lead to big consequences. J Proteome 75(16):4893–4911. doi:10.1016/j.jprot.2012.04.012
12. Stoeckli M, Staab D, Schweitzer A (2007) Compound and metabolite distribution measured by MALDI mass spectrometric imaging in whole-body tissue sections. Int J Mass Spectrom 260(2/3):195–202. doi:10.1016/j.ijms.2006.10.007
13. Hunag L (2002) Time-of-flight secondary ion mass spectrometry: quantitative approaches. Trends Vac Sci Technol 5:31–43
14. Stevie FA, Griffis DP (2008) Quantification in dynamic SIMS: current status and future needs. Appl Surf Sci 255(4):1364–1367. doi:10.1016/j.apsusc.2008.05.041
15. Werner HW (1980) Quantitative secondary ion mass spectrometry: a review. Surf Interface Anal 2(2):56–74. doi:10.1002/sia.740020205
16. Deng RC, Williams P (1989) Factors affecting precision and accuracy in quantitative analysis by secondary ion mass spectrometry. Anal Chem 61(17):1946–1948. doi:10.1021/ac00192a035
17. Seeley EH, Caprioli RM (2008) Molecular imaging of proteins in tissues by mass spectrometry. Proc Natl Acad Sci 105 (47):18126-18131. doi:10.1073/pnas.0801374105
18. Caprioli RM, Farmer TB, Gile J (1997) Molecular imaging of biological samples: localization of peptides and proteins using MALDI-TOF MS. Anal Chem 69(23):4751–4760. doi:10.1021/ac970888i
19. Stoeckli M, Schhaaf TG, Chaurand P, Caprioli RM (2001) Imaging mass spectrometry: a new technology for the analysis of protein expression in mammalian tissues. Nat Methods 7:493–496. doi:10.1038/86573
20. Chaurand P, Schwartz SA, Caprioli RM (2002) Imaging mass spectrometry: a new tool to investigate the spatial organization of peptides and proteins in mammalian tissue sections. Curr Opin Chem Biol 6(5):676–681. doi:10.1016/S1367-5931(02)00370-8
21. Chaurand P, Norris JL, Cornett DS, Mobley JA, Caprioli RM (2006) New developments in profiling and imaging of proteins from tissue sections by MALDI mass spectrometry. J Proteome Res 5(11):2889–2900. doi:10.1021/pr060346u
22. Greer T, Sturm R, Li L (2011) Mass spectrometry imaging for drugs and metabolites. J Proteom 74(12):2617–2631. doi:10.1016/j.jprot.2011.03.032
23. Zemski Berry KA, Hankin JA, Barkley RM, Spraggins JM, Caprioli RM, Murphy RC (2011) MALDI imaging of lipid biochemistry in tissues by mass spectrometry. Chem Rev 111(10):6491–6512. doi:10.1021/cr200280p

24. Touboul D, Brunelle A, Laprevote O (2011) Mass spectrometry imaging: towards a lipid microscope? Biochimie 93(1):113–119. doi:10.1016/j.biochi.2010.05.013
25. Sugiura Y, Setou M (2010) Imaging mass spectrometry for visualization of drug and endogenous metabolite distribution: toward in situ pharmacometabolomes. J NeuroImmune Pharmacol 5(1):31–43. doi:10.1007/s11481-009-9162-6
26. Trim P, Francese S, Clench M (2009) Imaging mass spectrometry for the assessment of drugs and metabolites in tissue. Bioanalysis 1(2):309–319. doi:10.4155/bio.09.33
27. Cornett DS, Reyzer ML, Chaurand P, Caprioli RM (2007) MALDI imaging mass spectrometry: molecular snapshots of biochemical systems. Nat Methods 4(10):828–833. doi:10.1038/nmeth1094
28. Walch A, Rauser S, Deininger S-O, Höfler H (2008) MALDI imaging mass spectrometry for direct tissue analysis: a new frontier for molecular histology. Histochem Cell Biol 130(3):421–434. doi:10.1007/s00418-008-0469-9
29. Balluff B, Schöne C, Höfler H, Walch A (2011) MALDI imaging mass spectrometry for direct tissue analysis: technological advancements and recent applications. Histochem Cell Biol 136(3):227–244. doi:10.1007/s00418-011-0843-x
30. Dreisewerd K (2003) The desorption process in MALDI. Chem Rev 103(2):395–426. doi:10.1021/cr010375i
31. Knochenmuss R (2006) Ion formation mechanisms in UV-MALDI. Analyst 131(9):966–986. doi:10.1039/B605646F
32. Aerni H-R, Cornett DS, Caprioli RM (2005) Automated acoustic matrix deposition for MALDI sample preparation. Anal Chem 78(3):827–834. doi:10.1021/ac051534r
33. Chen Y, Allegood J, Liu Y, Wang E, Cachon-Gonzalez B, Cox TM, Merrill AH, Sullards MC (2008) Imaging MALDI mass spectrometry using an oscillating capillary nebulizer matrix coating system and its application to analysis of lipids in brain from a mouse model of Tay-Sachs/Sandhoff disease. Anal Chem 80(8):2780–2788. doi:10.1021/ac702350g
34. Baluya DL, Garrett TJ, Yost RA (2007) Automated MALDI matrix deposition method with inkjet printing for imaging mass spectrometry. Anal Chem 79(17):6862–6867. doi:10.1021/ac070958d
35. Hankin JA, Barkley RM, Murphy RC (2007) Sublimation as a method of matrix application for mass spectrometric imaging. J Am Soc Mass Spectrom 18(9):1646–1652. doi:10.1016/j.jasms.2007.06.010
36. Puolitaival S, Burnum K, Cornett DS, Caprioli R (2008) Solvent-free matrix dry-coating for MALDI imaging of phospholipids. J Am Soc Mass Spectrom 19(6):882–886. doi:10.1016/j.jasms.2008.02.013
37. Li YL, Gross ML (2004) Ionic-liquid matrices for quantitative analysis by MALDI-TOF mass spectrometry. J Am Soc Mass Spectrom 15(12):1833–1837. doi:10.1016/j.jasms.2004.08.011
38. Zabet-Moghaddam M, Heinzle E, Tholey A (2004) Qualitative and quantitative analysis of low molecular weight compounds by ultraviolet matrix-assisted laser desorption/ionization mass spectrometry using ionic liquid matrices. Rapid Commun Mass Spectrom 18(2):141–148. doi:10.1002/rcm.1293
39. Bonnel D, Franck J, Mériaux C, Salzet M, Fournier I (2013) Ionic matrices pre-spotted matrix-assisted laser desorption/ionization plates for patient maker following in course of treatment, drug titration, and MALDI mass spectrometry imaging. Anal Biochem 434(1):187–198. doi:10.1016/j.ab.2012.10.035
40. Goodwin RJA, Scullion P, MacIntyre L, Watson DG, Pitt AR (2010) Use of a solvent-free dry matrix coating for quantitative matrix-assisted laser desorption ionization imaging of 4-bromophenyl-1,4-diazabicyclo(3.2.2)nonane-4-carboxylate in rat brain and quantitative analysis of the drug from laser microdissected tissue regions. Anal Chem 82(9):3868–3873. doi:10.1021/ac100398y
41. Signor L, Varesio E, Staack RF, Starke V, Richter WF, Hopfgartner G (2007) Analysis of erlotinib and its metabolites in rat tissue sections by MALDI quadrupole time-of-flight mass spectrometry. J Mass Spectrom 42(7):900–909. doi:10.1002/jms.1225
42. Luxembourg SL, McDonnell LA, Duursma MC, Guo X, Heeren RMA (2003) Effect of local matrix crystal variations in matrix-assisted ionization techniques for mass spectrometry. Anal Chem 75(10):2333–2341. doi:10.1021/ac026434p
43. Pachuta SJ, Cooks RG (1987) Mechanisms in molecular SIMS. Chem Rev 87(3):647–669. doi:10.1021/cr00079a009
44. Werner HW (1975) The use of secondary ion mass spectrometry in surface analysis. Surf Sci 47(1):301–323. doi:10.1016/0039-6028(75)90297-6
45. Vickerman JC (1994) Impact of mass spectrometry in surface analysis. Analyst 119(4):513–523. doi:10.1039/AN9941900513
46. Zoriy MV, Becker JS (2007) Imaging of elements in thin cross sections of human brain samples by LA-ICP-MS: a study on reproducibility. Int J Mass Spectrom 264(2/3):175–180. doi:10.1016/j.ijms.2007.04.009
47. Pisonero J, Fernandez B, Gunther D (2009) Critical revision of GD-MS, LA-ICP-MS, and SIMS as inorganic mass spectrometric techniques for direct solid analysis. J Anal At Spectrom 24(9):1145–1160. doi:10.1039/b904698d
48. Hare D, Austin C, Doble P (2012) Quantification strategies for elemental imaging of biological samples using laser ablation-inductively coupled plasma-mass spectrometry. Analyst 137(7):1527–1537. doi:10.1039/C2AN15792F
49. Sabine Becker J (2013) Imaging of metals in biological tissue by laser ablation inductively coupled plasma mass spectrometry (LA-ICP-MS): state of the art and future developments. J Mass Spectrom 48(2):255–268. doi:10.1002/jms.3168
50. Becker JS, Matusch A, Becker JS, Wu B, Palm C, Becker AJ, Salber D (2011) Mass spectrometric imaging (MSI) of metals using advanced BrainMet techniques for biomedical research. Int J Mass Spectrom 307(1/3):3–15. doi:10.1016/j.ijms.2011.01.015
51. Austin C, Fryer F, Lear J, Bishop D, Hare D, Rawling T, Kirkup L, McDonagh A, Doble P (2011) Factors affecting internal standard selection for quantitative elemental bio-imaging of soft tissues by LA-ICP-MS. J Anal At Spectrom 26(7):1494–1501. doi:10.1039/C0JA00267D
52. Konz I, Fernández B, Fernández ML, Pereiro R, Sanz-Medel A (2012) Laser ablation ICP-MS for quantitative biomedical applications. Anal Bioanal Chem 403(8):2113–2125. doi:10.1007/s00216-012-6023-6
53. Takáts Z, Wiseman JM, Gologan B, Cooks RG (2004) Mass spectrometry sampling under ambient conditions with desorption electrospray ionization. Science 306(5695):471–473. doi:10.1126/science.1104404
54. Monge ME, Harris GA, Dwivedi P, Fernández FM (2013) Mass spectrometry: recent advances in direct open air surface sampling/ionization. Chem Rev 113 (4):2269-2308. doi:10.1021/cr300309q
55. Van Berkel GJ, Pasilis SP, Ovchinnikova O (2008) Established and emerging atmospheric pressure surface sampling/ionization techniques for mass spectrometry. J Mass Spectrom 43(9):1161–1180. doi:10.1002/jms.1440
56. Harris GA, Galhena AS, Fernandez FM (2011) Ambient sampling/ionization mass spectrometry: applications and current trends. Anal Chem 83(12):4508–4538. doi:10.1021/ac200918u
57. Huang M-Z, Yuan C-H, Cheng S-C, Cho Y-T, Shiea J (2010) Ambient ionization mass spectrometry. Annu Rev Anal Chem 3(1):43–65. doi:10.1146/annurev.anchem.111808.073702
58. Ellis SR, Wu C, Deeley JM, Zhu X, Truscott RJW, in het Panhuis M, Cooks RG, Mitchell TW, Blanksby SJ (2010) Imaging of human lens lipids by desorption electrospray ionization mass spectrometry. J Am Soc Mass Spectrom 21(12):2095–2104. doi:10.1016/j.jasms.2010.09.003
59. Eberlin LS, Ferreira CR, Dill AL, Ifa DR, Cheng L, Cooks RG (2011) Nondestructive, histologically compatible tissue imaging by

desorption electrospray ionization mass spectrometry. ChemBioChem 12(14):2129–2132. doi:10.1002/cbic.201100411
60. Källback P, Shariatgorji M, Nilsson A, Andrén PE (2012) Novel mass spectrometry imaging software assisting labeled normalization and quantitation of drugs and neuropeptides directly in tissue sections. J Proteom 75(16):4941–4951. doi:10.1016/j.jprot.2012.07.034
61. Chandra S (2010) Quantitative imaging of chemical composition in single cells by secondary ion mass spectrometry: cisplatin affects calcium stores in renal epithelial cells. In: Rubakhin SS, Sweedler JV (eds) Mass spectrometry imaging, vol 656. Methods in molecular biology. Humana Press: pp 113–130. doi:10.1007/978-1-60761-746-4_6
62. Dérue C, Gibouin D, Lefebvre F, Studer D, Thellier M, Ripoll C (2006) Relative sensitivity factors of inorganic cations in frozen-hydrated standards in secondary ion MS analysis. Anal Chem 78(8): 2471–2477. doi:10.1021/ac051518u
63. Smith DR, Chandra S, Barth RF, Yang W, Joel DD, Coderre JA (2001) Quantitative imaging and microlocalization of boron-10 in brain tumors and infiltrating tumor cells by SIMS ion microscopy: relevance to neutron capture therapy. Cancer Res 61(22):8179–8187
64. Candy JM, Oakley AE, Mountfort SA, Taylor GA, Morris CM, Bishop HE, Edwardson JA (1992) The imaging and quantification of aluminium in the human brain using dynamic secondary ion mass spectrometry (SIMS). Biol Cell 74(1):109–118. doi:10.1016/0248-4900(92)90016-t
65. Ausserer WA, Ling YC, Chandra S, Morrison GH (1989) Quantitative imaging of boron, calcium, magnesium, potassium, and sodium distributions in cultured cells with ion microscopy. Anal Chem 61(24):2690–2695. doi:10.1021/ac00199a002
66. Chandra S, Tjarks W, Lorey DR, Barth RF (2008) Quantitative subcellular imaging of boron compounds in individual mitotic and interphase human glioblastoma cells with imaging secondary ion mass spectrometry (SIMS). J Microsc 229(1):92–103. doi:10.1111/j.1365-2818.2007.01869.x
67. Chandra S, Kabalka GW, Lorey DR, Smith DR, Coderre JA (2002) Imaging of fluorine and boron from fluorinated boronophenylalanine in the same cell at organelle resolution by correlative ion microscopy and confocal laser scanning microscopy. Clin Cancer Res 8(8):2675–2683
68. Harris WC, Chandra S, Morrison GH (1983) Ion implantation for quantitative ion microscopy of biological soft tissue. Anal Chem 55(12):1959–1963. doi:10.1021/ac00262a029
69. Vismeh R, Waldon DJ, Teffera Y, Zhao Z (2012) Localization and quantification of drugs in animal tissues by use of desorption electrospray ionization mass spectrometry imaging. Anal Chem 84(12):5439–5445. doi:10.1021/ac3011654
70. Pirman DA, Yost RA (2011) Quantitative tandem mass spectrometric imaging of endogenous acetyl-l-carnitine from piglet brain tissue using an internal standard. Anal Chem 83(22):8575–8581. doi:10.1021/ac201949b
71. Pirman DA, Kiss A, Heeren RMA, Yost RA (2012) Identifying tissue-specific signal variation in MALDI mass spectrometric imaging by use of an internal standard. Anal Chem 85(2):1090–1096. doi:10.1021/ac3029618
72. Pirman DA, Reich RF, Kiss A, Heeren RMA, Yost RA (2012) Quantitative MALDI tandem mass spectrometric imaging of cocaine from brain tissue with a deuterated internal standard. Anal Chem 85(2):1081–1089. doi:10.1021/ac302960j
73. Nilsson A, Fehniger TE, Gustavsson L, Andersson M, Kenne K, Marko-Varga G, Andrén PE (2010) Fine mapping the spatial distribution and concentration of unlabeled drugs within tissue microcompartments using imaging mass spectrometry. PLoS ONE 5(7): e11411. doi:10.1371/journal.pone.0011411
74. Clemis EJ, Smith DS, Camenzind AG, Danell RM, Parker CE, Borchers CH (2012) Quantitation of spatially-localized proteins in tissue samples using MALDI-MRM imaging. Anal Chem 84(8): 3514–3522. doi:10.1021/ac202875d
75. Hamm G, Bonnel D, Legouffe R, Pamelard F, Delbos J-M, Bouzom F, Stauber J (2012) Quantitative mass spectrometry imaging of propranolol and olanzapine using tissue extinction calculation as normalization factor. J Proteom 75(16):4952–4961. doi:10.1016/j.jprot.2012.07.035
76. Koeniger SL, Talaty N, Luo Y, Ready D, Voorbach M, Seifert T, Cepa S, Fagerland JA, Bouska J, Buck W, Johnson RW, Spanton S (2011) A quantitation method for mass spectrometry imaging. Rapid Commun Mass Spectrom 25(4):503–510. doi:10.1002/rcm.4891
77. Groseclose MR, Castellino S (2013) A mimetic tissue model for the quantification of drug distributions by MALDI imaging mass spectrometry. Anal Chem 85 (21):10099-10106. doi:10.1021/ac400892z
78. Kindness A, Sekaran CN, Feldmann J (2003) Two-dimensional mapping of copper and zinc in liver sections by laser ablation-inductively coupled plasma mass spectrometry. Clin Chem 49(11): 1916–1923. doi:10.1373/clinchem.2003.022046
79. Jackson B, Harper S, Smith L, Flinn J (2006) Elemental mapping and quantitative analysis of Cu, Zn, and Fe in rat brain sections by laser ablation ICP-MS. Anal Bioanal Chem 384(4):951–957. doi:10.1007/s00216-005-0264-6
80. Feldmann J, Kindness A, Ek P (2002) Laser ablation of soft tissue using a cryogenically cooled ablation cell. J Anal At Spectrom 17(8):813–818. doi:10.1039/B201960D
81. Hare DJ, George JL, Grimm R, Wilkins S, Adlard PA, Cherny RA, Bush AI, Finkelstein DI, Doble P (2010) Three-dimensional elemental bio-imaging of Fe, Zn, Cu, Mn, and P in a 6-hydroxydopamine lesioned mouse brain. Metallomics 2(11):745–753. doi:10.1039/c0mt00039f
82. Matusch A, Bauer A, Becker JS (2011) Element imaging in formalin fixed slices of human mesencephalon. Int J Mass Spectrom 307(1/3):240–244. doi:10.1016/j.ijms.2011.03.006
83. Matusch A, Depboylu C, Palm C, Wu B, Höglinger G, Schäfer MH, Becker JS (2010) Cerebral bioimaging of Cu, Fe, Zn, and Mn in the MPTP mouse model of Parkinson's disease using laser ablation inductively coupled plasma mass spectrometry (LA-ICP-MS). J Am Soc Mass Spectrom 21(1):161–171. doi:10.1016/j.jasms.2009.09.022
84. Austin C, Hare D, Rawling T, McDonagh AM, Doble P (2010) Quantification method for elemental bio-imaging by LA-ICP-MS using metal spiked PMMA films. J Anal At Spectrom 25(5):722–725. doi:10.1039/B911316A
85. Becker JS, Zoriy M, Becker JS, Dobrowolska J, Dehnhardt M, Matusch A (2007) Elemental imaging mass spectrometry of thin sections of tissues and analysis of brain proteins in gels by laser ablation inductively coupled plasma mass spectrometry. Phys Status Solidi 4(6):1775–1784. doi:10.1002/pssc.200675226
86. Zoriy MV, Dehnhardt M, Matusch A, Becker JS (2008) Comparative imaging of P, S, Fe, Cu, Zn, and C in thin sections of rat brain tumor as well as control tissues by laser ablation inductively coupled plasma mass spectrometry. Spectrochim Acta B Atomic Spectrosc 63(3):375–382. doi:10.1016/j.sab.2007.11.030
87. Dobrowolska J, Dehnhardt M, Matusch A, Zoriy M, Palomero-Gallagher N, Koscielniak P, Zilles K, Becker JS (2008) Quantitative imaging of zinc, copper, and lead in three distinct regions of the human brain by laser ablation inductively coupled plasma mass spectrometry. Talanta 74(4):717–723. doi:10.1016/j.talanta.2007.06.051
88. Zoriy MV, Dehnhardt M, Reifenberger G, Zilles K, Becker JS (2006) Imaging of Cu, Zn, Pb, and U in human brain tumor resections by laser ablation inductively coupled plasma mass spectrometry. Int J Mass Spectrom 257(1/3):27–33. doi:10.1016/j.ijms.2006.06.005

89. Drescher D, Giesen C, Traub H, Panne U, Kneipp J, Jakubowski N (2012) Quantitative imaging of gold and silver nanoparticles in single eukaryotic cells by laser ablation ICP-MS. Anal Chem 84(22):9684–9688. doi:10.1021/ac302639c
90. Becker JS, Zoriy MV, Pickhardt C, Palomero-Gallagher N, Zilles K (2005) Imaging of copper, zinc, and other elements in thin section of human brain samples (hippocampus) by laser ablation inductively coupled plasma mass spectrometry. Anal Chem 77(10):3208–3216. doi:10.1021/ac040184q
91. Bellis DJ, Santamaria-Fernandez R (2010) Ink jet patterns as model samples for the development of LA-ICP-SFMS methodology for mapping of elemental distribution with reference to biological samples. J Anal At Spectrom 25(7):957–963. doi:10.1039/B926430B
92. Hare D, Austin C, Doble P, Arora M (2011) Elemental bio-imaging of trace elements in teeth using laser ablation-inductively coupled plasma-mass spectrometry. J Dent 39(5):397–403. doi:10.1016/j.jdent.2011.03.004
93. M-M P, Weiskirchen R, Gassler N, Bosserhoff AK, Becker JS (2013) Novel bioimaging techniques of metals by laser ablation inductively coupled plasma mass spectrometry for diagnosis of fibrotic and cirrhotic liver disorders. PLoS ONE 8(3):e58702. doi:10.1371/journal.pone.0058702
94. Pozebon D, Dressler VL, Mesko MF, Matusch A, Becker JS (2010) Bioimaging of metals in thin mouse brain section by laser ablation inductively coupled plasma mass spectrometry: novel online quantification strategy using aqueous standards. J Anal At Spectrom 25(11):1739–1744. doi:10.1039/c0ja00055h
95. Gunther D, Cousin H, Magyar B, Leopold I (1997) Calibration studies on dried aerosols for laser ablation-inductively coupled plasma mass spectrometry. J Anal At Spectrom 12(2):165–170. doi:10.1039/A604531F
96. Hare D, Reedy B, Grimm R, Wilkins S, Volitakis I, George JL, Cherny RA, Bush AI, Finkelstein DI, Doble P (2009) Quantitative elemental bio-imaging of Mn, Fe, Cu, and Zn in 6-hydroxydopamine induced Parkinsonism mouse models. Metallomics 1(1):53–58. doi:10.1039/b816188g
97. Dressler VL, Pozebon D, Mesko MF, Matusch A, Kumtabtim U, Wu B, Sabine Becker J (2010) Biomonitoring of essential and toxic metals in single hair using on-line solution-based calibration in laser ablation inductively coupled plasma mass spectrometry. Talanta 82(5):1770–1777. doi:10.1016/j.talanta.2010.07.065
98. Sussulini A, Wiener E, Marnitz T, Wu B, Müller B, Hamm B, Sabine Becker J (2013) Quantitative imaging of the tissue contrast agent [Gd(DTPA)]2− in articular cartilage by laser ablation inductively coupled plasma mass spectrometry. Contrast Media Mol Imaging 8(2):204–209. doi:10.1002/cmmi.1509
99. Boulyga SF, Desideri D, Meli MA, Testa C, Becker JS (2003) Plutonium and americium determination in mosses by laser ablation ICP-MS combined with isotope dilution technique. Int J Mass Spectrom 226(3):329–339. doi:10.1016/S1387-3806(03)00024-1
100. Arlinghaus HF, Kriegeskotte C, Fartmann M, Wittig A, Sauerwein W, Lipinsky D (2006) Mass spectrometric characterization of elements and molecules in cell cultures and tissues. Appl Surf Sci 252(19):6941–6948. doi:10.1016/j.apsusc.2006.02.186
101. Fartmann M, Kriegeskotte C, Dambach S, Wittig A, Sauerwein W, Arlinghaus HF (2004) Quantitative imaging of atomic and molecular species in cancer cell cultures with TOF-SIMS and laser-SNMS. Appl Surf Sci 231/232(0):428–431. doi:10.1016/j.apsusc.2004.03.160
102. Strick R, Strissel PL, Gavrilov K, Levi-Setti R (2001) Cation–chromatin binding as shown by ion microscopy is essential for the structural integrity of chromosomes. J Cell Biol 155(6):899–910. doi:10.1083/jcb.200105026
103. Jackson LM, Hue JJ, Winograd N (2013) Quantitative detection of purines in biologically relevant films with TOF-secondary ion mass spectrometry. Surf Interface Anal 45(1):237–239. doi:10.1002/sia.5098
104. Gillen G, Hues SM (1993) Doped gelatin films as a model matrix for molecular secondary ion mass spectrometry studies of biological soft tissue. J Am Soc Mass Spectrom 4(5):419–423. doi:10.1016/1044-0305(93)85007-K
105. Tibi M, Heumann KG (2003) Isotope dilution mass spectrometry as a calibration method for the analysis of trace elements in powder samples by LA-ICP-MS. J Anal At Spectrom 18(9):1076–1081. doi:10.1039/B301835K
106. Pickhardt C, Izmer AV, Zoriy MV, Schaumlöffel D, Sabine Becker J (2006) On-line isotope dilution in laser ablation inductively coupled plasma mass spectrometry using a microflow nebulizer inserted in the laser ablation chamber. Int J Mass Spectrom 248(3):136–141. doi:10.1016/j.ijms.2005.11.001
107. Wang AZ, Langer R, Farokhzad OC (2012) Nanoparticle delivery of cancer drugs. Annu Rev Med 63(1):185–198. doi:10.1146/annurev-med-040210-162544
108. Aeschliman DB, Bajic SJ, Baldwin DP, Houk RS (2003) Spatially-resolved analysis of solids by laser ablation-inductively coupled plasma-mass spectrometry: trace elemental quantification without matrix-matched solid standards. J Anal At Spectrom 18(8):872–877. doi:10.1039/B205683F
109. Mitsuma T, Adachi K, Mukoyama M, Ohsugi K, Ando K (1988) Concentrations of thyrotropin-releasing hormone and Substance P are increased in several areas of the central nervous system of shambling mutant mice. Neurochem Int 13(2):261–264. doi:10.1016/0197-0186(88)90063-0
110. Drexler DM, Garrett TJ, Cantone JL, Diters RW, Mitroka JG, Prieto Conaway MC, Adams SP, Yost RA, Sanders M (2007) Utility of imaging mass spectrometry (IMS) by matrix-assisted laser desorption ionization (MALDI) on an ion trap mass spectrometer in the analysis of drugs and metabolites in biological tissues. J Pharmacol Toxicol Methods 55(3):279–288. doi:10.1016/j.vascn.2006.11.004
111. Kertesz V, Van Berkel GJ (2010) Fully automated liquid extraction-based surface sampling and ionization using a chip-based robotic nanoelectrospray platform. J Mass Spectrom 45(3):252–260. doi:10.1002/jms.1709
112. Van Berkel GJ, Kertesz V, Koeplinger KA, Vavrek M, Kong A-NT (2008) Liquid microjunction surface sampling probe electrospray mass spectrometry for detection of drugs and metabolites in thin tissue sections. J Mass Spectrom 43(4):500–508. doi:10.1002/jms.1340
113. McLean JA, Ridenour WB, Caprioli RM (2007) Profiling and imaging of tissues by imaging ion mobility-mass spectrometry. J Mass Spectrom 42(8):1099–1105. doi:10.1002/jms.1254
114. Kiss A, Heeren R (2011) Size, weight and position: ion mobility spectrometry and imaging MS combined. Anal Bioanal Chem 399(8):2623–2634. doi:10.1007/s00216-010-4644-1
115. Harris GA, Nyadong L, Fernandez FM (2008) Recent developments in ambient ionization techniques for analytical mass spectrometry. Analyst 133(10):1297–1301. doi:10.1039/B806810K
116. Imabiotech (2013) Available at: http://quantinetix-software.imabiotech.com/Quantinetix-TM.html. Accessed 23/4/2013